The Astrophysical Journal, 881:50 (6pp), 2019 August 10 https://doi.org/10.3847/1538-4357/ab2be9

On Exact Laws in Incompressible Hall Magnetohydrodynamic Turbulence

R. Ferrand[1], S. Galtier[1,2], F. Sahraoui[1], R. Meyrand[1], N. Andrés[1,3], and S. Banerjee[4]
[1] LPP/CNRS-Ecole polytechnique-Sorbonne Université-Université Paris-Sud-Observatoire de Paris, F-91128 Palaiseau, France; renaud.ferrand@lpp.polytechnique.fr
[2] Institut Universitaire de France, France
[3] Instituto de Astronomía y Física del Espacio, UBA-CONICET, CC. 67, suc. 28, 1428, Buenos Aires, Argentina
[4] Department of Physics, Indian Institute of Technology Kanpur, Kalyanpur 208016, Uttar Pradesh, India
Received 2019 May 10; revised 2019 June 20; accepted 2019 June 20; published 2019 August 12

Abstract

A comparison is made between several existing exact laws in incompressible Hall magnetohydrodynamic turbulence in order to show their equivalence, despite stemming from different mathematical derivations. Using statistical homogeneity, we revisit the law proposed by Hellinger et al. and show that it can be written, after being corrected by a multiplicative factor, in a more compact form implying only flux terms expressed as increments of the turbulent fields. The Hall contribution of this law is tested and compared to other exact laws derived by Galtier and Banerjee & Galtier using direct numerical simulations of three-dimensional electron MHD turbulence with a moderate mean magnetic field. We show that the studied laws are equivalent in the inertial range, thereby offering several choices on the formulation to use depending on the needs. The expressions that depend explicitly on a mean (guide) field may lead to residual errors in estimating the energy cascade rate; however, we demonstrate that this guide field can be removed from these laws after mathematical manipulation. Therefore, it is recommended to use an expression independent of the mean guide field to analyze numerical or in situ spacecraft data.

Key words: magnetohydrodynamics (MHD) – plasmas – solar wind – turbulence

1. Introduction

To date, understanding the dynamics of turbulent flows remains one of the most challenging problems of classical physics. As these systems are inherently chaotic they are generally studied by statistical means, thus requiring specific tools to be dealt with (Frisch 1995). The so-called exact laws are among the most important theoretical results of turbulence. The derivation of these statistical laws is based on the assumption of the existence of an inertial range where the physics is dominated by the nonlinear transfer from one scale to another. In a fully developed three-dimensional (3D) hydrodynamic turbulence of an incompressible fluid, kinetic energy is transferred from macroscopic length scales to the scale of molecular diffusion until it is eventually dissipated into thermal energy by viscous effects. The mean transfer rate of kinetic energy per unit volume, which is usually denoted by ε, is assumed to remain constant at each scale in the inertial range where both dissipation and forcing mechanisms are negligible. It is also equal to the average energy dissipation rate, which is expected to be independent of the viscosity in the limit of large Reynolds numbers. This property, often called the zeroth law of turbulence (Onsager 1949; Eyink 1994; Duchon & Robert 2000; Saint-Michel et al. 2014), is actually used to link the fluctuations of the velocity field to ε through exact laws.

The first and the most popular exact law is the so-called Kolmogorov's four-fifths law, which was derived for incompressible turbulence (Kolmogorov 1941). It was first derived using tensorial calculus (Batchelor 1953), but a similar four-thirds law was computed more directly through the dynamical study of an appropriate two-point correlation function (Monin 1959; Antonia et al. 1997). Using these methods (with the generalized zeroth law of turbulence; Mininni & Pouquet 2009; Bandyopadhyay et al. 2018; Galtier 2018), new laws were derived for different plasma models such as incompressible MHD (IMHD; Politano & Pouquet 1998a) or incompressible Hall magnetohydrodynamic (IHMHD; Galtier 2008). More recently, these results were extended to compressible (isothermal and polytropic) turbulence in hydrodynamics (CHD; Galtier & Banerjee 2011; Banerjee & Galtier 2014), and then to isothermal compressible MHD (CMHD; Banerjee & Galtier 2013; Andrés & Sahraoui 2017) and compressible HMHD (Andrés et al. 2018a). Using an alternative formulation (Banerjee & Galtier 2016, 2017), compressible exact relations were also derived for self-gravitating turbulence of both neutral and MHD fluids (Banerjee & Kritsuk 2017, 2018). Such laws were also derived for self-gravitating turbulence whose potential applications are the interstellar medium and star formation.

Since ε can be used as a proxy to evaluate the amount of energy available to be ultimately dissipated at small scales, exact laws are often used in collisionless astrophysical plasmas, such as the solar wind (SW), to evaluate the rate of plasma heating. Indeed, Richardson et al. (1995) have evidenced using *Voyager* data a slower decay of the (ion) temperature with the heliocentric distance in comparison with the prediction from the adiabatic expansion model (Matthaeus et al. 1999). Turbulence is proposed to explain this problem because it provides an efficient mechanism of energy dissipation through the nonlinear process of energy cascade from the MHD scales down to the sub-ion and electron scales, where the energy is eventually dissipated through some kinetic effects (Sahraoui et al. 2009, 2010; He et al. 2015). The energy cascade (or dissipation) rate was measured in both the SW (Podesta et al. 2007; Sorriso-Valvo et al. 2007; MacBride et al. 2008; Marino et al. 2008; Carbone et al. 2009; Smith et al. 2009; Stawarz et al. 2009; Osman et al. 2011; Coburn et al. 2015; Banerjee et al. 2016; Hadid et al. 2017) and the Earth's magnetosheath (Hadid et al. 2018), and was shown to enlighten many aspects related to the dynamics of turbulent space plasmas.

Similarly to hydrodynamics, the case of IHMHD has driven some attention over the past 10 years with the derivation of several exact laws (Galtier 2008; Banerjee & Galtier 2017; Hellinger et al. 2018). Although the underlying assumptions remain unchanged, these laws stem from the analysis of different statistical quantities. On the one hand, the laws given in Galtier (2008, hereafter G08) and Banerjee & Galtier (2017, hereafter BG17) are derived from the dynamical analysis of the two-point correlator:

$$\langle R_E\rangle = \left\langle \frac{\boldsymbol{v}\cdot\boldsymbol{v}' + \boldsymbol{b}\cdot\boldsymbol{b}'}{2}\right\rangle, \tag{1}$$

where $\langle\rangle$ is the ensemble average, $\boldsymbol{v}$ and $\boldsymbol{b}$ are the local velocity and Alfvén velocity fields, respectively, and the prime distinguishes values taken at points $\boldsymbol{x}$ and $\boldsymbol{x}'$, respectively (see Section 2 for the definitions). However, the calculation was done differently in the two models (G08 and BG17) and yielded quite different expressions that cannot be trivially connected to each other. On the other hand, the law from Hellinger et al. (2018, hereafter H18) stems from the evolution equation of the second-order structure function

$$\langle S\rangle = \langle|\boldsymbol{v}'-\boldsymbol{v}|^2 + |\boldsymbol{b}'-\boldsymbol{b}|^2\rangle, \tag{2}$$

which is linked to expression (1) through the relation $\langle S/4\rangle = \langle E^{\rm tot}\rangle - \langle R_E\rangle$ with $E^{\rm tot} = (\boldsymbol{v}^2+\boldsymbol{b}^2)/2$ the total energy. It is thus important to check whether or not these different laws are consistent with each other by providing the same energy cascade rate. Note that in the definition (2), $\langle S\rangle$ is independent of the (constant) mean fields $\boldsymbol{v}_0$ and $\boldsymbol{b}_0$. We will return to this point in Section 5.

This paper aims at studying analytically and numerically the IHMHD exact laws and checking if they are mathematically equivalent despite stemming from a different logic of derivation. Following this goal, we expose in Section 2 a rigorous derivation of H18 and find a slight difference with the original paper. Furthermore, we provide a new, more compact form of that law that depends only on flux terms (hereafter F19). In Section 4 we give mathematical proof of the equivalence of the three laws F19, G08, and BG17. This equivalence is eventually tested in Section 5 with 3D direct numerical simulations (DNSs) of electron MHD (EMHD) turbulence. We also discuss the possible influence of a mean magnetic field on the exact laws and on the methods used to evaluate the energy cascade rate. The results are summarized and discussed in Section 6.

2. Derivation of H18

In this section we propose a step-by-step derivation of the H18 law based on the same premises as in the original paper, where the details were not given. Let $\boldsymbol{B}$ represent the magnetic field and $\boldsymbol{J} = \boldsymbol{\nabla}\times\boldsymbol{B}/\mu_0$ represent the electric current; the mass density ρ_0 is taken constant and equal to unity. We use the Alfvén units for the magnetic field and the electric current, i.e., $\boldsymbol{b} = \boldsymbol{B}/\sqrt{\mu_0\rho_0}$ and $\boldsymbol{j} = \boldsymbol{\nabla}\times\boldsymbol{b}$. In the incompressible case (i.e., $\boldsymbol{\nabla}\cdot\boldsymbol{v} = 0$) we get the following velocity and induction equations:

$$\partial_t\boldsymbol{v} = -(\boldsymbol{v}\cdot\boldsymbol{\nabla})\boldsymbol{v} + (\boldsymbol{b}\cdot\boldsymbol{\nabla})\boldsymbol{b} - \boldsymbol{\nabla}P + \boldsymbol{d}_\nu + \boldsymbol{f},$$

$$\partial_t\boldsymbol{b} = -(\boldsymbol{v}\cdot\boldsymbol{\nabla})\boldsymbol{b} + (\boldsymbol{b}\cdot\boldsymbol{\nabla})\boldsymbol{v} \tag{3}$$

$$+d_i(\boldsymbol{j}\cdot\boldsymbol{\nabla})\boldsymbol{b} - d_i(\boldsymbol{b}\cdot\boldsymbol{\nabla})\boldsymbol{j} + \boldsymbol{d}_\eta, \tag{4}$$

$$\boldsymbol{\nabla}\cdot\boldsymbol{b} = 0, \tag{5}$$

where $P = p + b^2/2$ is the total pressure, d_i the ion inertial length, and $\boldsymbol{f}$ a stationary homogeneous external force acting at large scales. The dissipation terms are

$$\boldsymbol{d}_\nu = \nu\Delta\boldsymbol{v}, \tag{6}$$

$$\boldsymbol{d}_\eta = \eta\Delta\boldsymbol{b}, \tag{7}$$

where ν is the kinematic viscosity and η the magnetic diffusivity. For this system the equation of total energy conservation writes (Galtier 2016)

$$\partial_t\langle E^{\rm tot}\rangle = \langle\boldsymbol{v}\cdot\boldsymbol{d}_\nu\rangle + \langle\boldsymbol{b}\cdot\boldsymbol{d}_\eta\rangle + \langle\boldsymbol{v}\cdot\boldsymbol{f}\rangle, \tag{8}$$

where $\langle\rangle$ is an ensemble average, which is equivalent to a spatial average in homogeneous turbulence. We define the mean rate of total energy injection as $\varepsilon = \langle\boldsymbol{v}\cdot\boldsymbol{f}\rangle$. With this, we can conclude that in the stationary regime the following relation holds: $\langle\boldsymbol{v}\cdot\boldsymbol{d}_\nu + \boldsymbol{b}\cdot\boldsymbol{d}_\eta\rangle = -\varepsilon$. Note that using the relation $\langle\boldsymbol{X}\cdot\Delta\boldsymbol{X}\rangle = -\langle(\boldsymbol{\nabla}\times\boldsymbol{X})^2\rangle$, which is valid for any incompressible vector field $\boldsymbol{X}$, we also have

$$\langle\boldsymbol{v}\cdot\boldsymbol{d}_\nu\rangle + \langle\boldsymbol{b}\cdot\boldsymbol{d}_\eta\rangle = -\nu\langle\boldsymbol{w}^2\rangle - \eta\langle\boldsymbol{j}^2\rangle, \tag{9}$$

with $\boldsymbol{w} = \nabla\times\boldsymbol{v}$ the vorticity, which gives the expression of the mean rate of total energy dissipation.

Next, we consider a spatial increment $\boldsymbol{\ell}$ connecting two points in space $\boldsymbol{x}$ and $\boldsymbol{x}'$, as $\boldsymbol{x}' = \boldsymbol{x} + \boldsymbol{\ell}$, and we define $\boldsymbol{v}\equiv\boldsymbol{v}(\boldsymbol{x})$ and $\boldsymbol{v}'\equiv\boldsymbol{v}(\boldsymbol{x}')$; the same notation is used for other variables. We also define the velocity increment $\delta\boldsymbol{v}\equiv\boldsymbol{v}'-\boldsymbol{v}$. We recall that under this formalism, we have for any entity A: $\partial_x A' = \partial_{x'}A = 0$. We then search for a dynamical equation for expression (2), under the hypothesis of statistical homogeneity, which means that we have to calculate $\partial_t\langle S\rangle$. Using Equations (3)–(5) and the incompressibility of the flow we obtain

$$\partial_t\boldsymbol{v}^2 = -\boldsymbol{\nabla}\cdot[(\boldsymbol{v}\cdot\boldsymbol{v})\boldsymbol{v}] + 2\boldsymbol{v}\cdot(\boldsymbol{b}\cdot\boldsymbol{\nabla})\boldsymbol{b} - 2\boldsymbol{v}\cdot\boldsymbol{\nabla}P + 2\boldsymbol{v}\cdot\boldsymbol{d}_\nu + 2\boldsymbol{v}\cdot\boldsymbol{f}, \tag{10}$$

$$\partial_t\boldsymbol{b}^2 = -\boldsymbol{\nabla}\cdot[(\boldsymbol{b}\cdot\boldsymbol{b})\boldsymbol{v}] + 2\boldsymbol{b}\cdot(\boldsymbol{b}\cdot\boldsymbol{\nabla})\boldsymbol{v} + d_i\boldsymbol{\nabla}\cdot[(\boldsymbol{b}\cdot\boldsymbol{b})\boldsymbol{j}] - 2d_i\boldsymbol{b}(\boldsymbol{b}\cdot\boldsymbol{\nabla})\boldsymbol{j} + 2\boldsymbol{b}\cdot\boldsymbol{d}_\eta, \tag{11}$$

$$\partial_t(\boldsymbol{v}\cdot\boldsymbol{v}') = -\boldsymbol{\nabla}'\cdot[(\boldsymbol{v}\cdot\boldsymbol{v}')\boldsymbol{v}' - (\boldsymbol{v}\cdot\boldsymbol{b}')\boldsymbol{b}' + P'\boldsymbol{v}] - \boldsymbol{\nabla}\cdot[(\boldsymbol{v}\cdot\boldsymbol{v}')\boldsymbol{v} - (\boldsymbol{v}'\cdot\boldsymbol{b})\boldsymbol{b} + P\boldsymbol{v}'] + \boldsymbol{v}'\cdot\boldsymbol{d}_\nu + \boldsymbol{v}\cdot\boldsymbol{d}'_\nu + \boldsymbol{v}'\cdot\boldsymbol{f} + \boldsymbol{v}\cdot\boldsymbol{f}', \tag{12}$$

$$\partial_t(\boldsymbol{b}\cdot\boldsymbol{b}') = -\boldsymbol{\nabla}'\cdot[(\boldsymbol{b}\cdot\boldsymbol{b}')\boldsymbol{v}' - (\boldsymbol{b}\cdot\boldsymbol{v}')\boldsymbol{b}' - d_i(\boldsymbol{b}\cdot\boldsymbol{b}')\boldsymbol{j}' + d_i(\boldsymbol{b}\cdot\boldsymbol{j}')\boldsymbol{b}'] - \boldsymbol{\nabla}\cdot[(\boldsymbol{b}'\cdot\boldsymbol{b})\boldsymbol{v} - (\boldsymbol{b}'\cdot\boldsymbol{v})\boldsymbol{b} - d_i(\boldsymbol{b}'\cdot\boldsymbol{b})\boldsymbol{j} + d_i(\boldsymbol{b}'\cdot\boldsymbol{j})\boldsymbol{b}] + \boldsymbol{b}'\cdot\boldsymbol{d}_\eta + \boldsymbol{b}\cdot\boldsymbol{d}'_\eta, \tag{13}$$

and similar equations as Equations (10)–(11) for the primed expressions. Below we will consider the ensemble average of the previous equations. We can use the relation $\langle\boldsymbol{\nabla}'\cdot\rangle = -\langle\boldsymbol{\nabla}\cdot\rangle = \boldsymbol{\nabla}_\ell\cdot\langle\rangle$, where $\boldsymbol{\nabla}_\ell$ denotes the derivative operator along the increment $\boldsymbol{\ell}$, to suppress the pressure terms in Equations (10) and (12):

$$\langle\boldsymbol{v}\cdot\boldsymbol{\nabla}P\rangle = \langle\boldsymbol{\nabla}\cdot(P\boldsymbol{v})\rangle = -\langle\boldsymbol{\nabla}'\cdot(P\boldsymbol{v})\rangle = 0,$$

$$\langle\boldsymbol{\nabla}'\cdot(P'\boldsymbol{v})\rangle = -\langle\boldsymbol{\nabla}\cdot(P'\boldsymbol{v})\rangle = 0.$$

By remarking that

$$\langle \boldsymbol{v} \cdot (\boldsymbol{b} \cdot \nabla)\boldsymbol{b} \rangle = -\langle \boldsymbol{b} \cdot (\boldsymbol{b} \cdot \nabla)\boldsymbol{v} \rangle,$$
$$\langle \boldsymbol{b} \cdot (\boldsymbol{b} \cdot \nabla)\boldsymbol{j} \rangle = -\langle \boldsymbol{j} \cdot (\boldsymbol{b} \cdot \nabla)\boldsymbol{b} \rangle,$$

a combination of Equations (10)–(13) leads to

$$\begin{aligned}
\partial_t \langle S \rangle = &\\
& 2\nabla_\ell \cdot \langle (\boldsymbol{v} \cdot \boldsymbol{v}')\delta\boldsymbol{v} + (\boldsymbol{b} \cdot \boldsymbol{b}')\delta\boldsymbol{v} \\
& - (\boldsymbol{v} \cdot \boldsymbol{b}')\delta\boldsymbol{b} - (\boldsymbol{b} \cdot \boldsymbol{v}')\delta\boldsymbol{b} \rangle \\
& + 2d_i \nabla_\ell \cdot \langle -(\boldsymbol{b} \cdot \boldsymbol{b}')\delta\boldsymbol{j} + (\boldsymbol{b} \cdot \boldsymbol{j}')\boldsymbol{b}' - (\boldsymbol{b}' \cdot \boldsymbol{j})\boldsymbol{b} \rangle \\
& + 2d_i \langle \boldsymbol{j} \cdot (\boldsymbol{b} \cdot \nabla)\boldsymbol{b} + \boldsymbol{j}' \cdot (\boldsymbol{b}' \cdot \nabla')\boldsymbol{b}' \rangle \\
& + 4\langle \boldsymbol{v} \cdot \boldsymbol{d}_\nu \rangle - 2\langle \boldsymbol{v} \cdot \boldsymbol{d'}_\nu \rangle - 2\langle \boldsymbol{v}' \cdot \boldsymbol{d}_\nu \rangle + 4\langle \boldsymbol{b} \cdot \boldsymbol{d}_\eta \rangle \\
& - 2\langle \boldsymbol{b} \cdot \boldsymbol{d'}_\eta \rangle - 2\langle \boldsymbol{b}' \cdot \boldsymbol{d}_\eta \rangle + 4\langle \boldsymbol{v} \cdot \boldsymbol{f} \rangle \\
& - 2\langle \boldsymbol{v} \cdot \boldsymbol{f}' \rangle - 2\langle \boldsymbol{v}' \cdot \boldsymbol{f} \rangle.
\end{aligned} \tag{14}$$

To further simplify expression (14) we can use the equalities $\nabla \cdot [(\boldsymbol{b} \cdot \boldsymbol{j}')\boldsymbol{b}] = \boldsymbol{j}' \cdot (\boldsymbol{b} \cdot \nabla)\boldsymbol{b}$ and $\nabla' \cdot [(\boldsymbol{b}' \cdot \boldsymbol{j})\boldsymbol{b}'] = \boldsymbol{j} \cdot (\boldsymbol{b}' \cdot \nabla')\boldsymbol{b}'$ and relation (8). We then obtain

$$\begin{aligned}
\partial_t \langle S \rangle = & -\nabla_\ell \cdot \langle (\delta\boldsymbol{v} \cdot \delta\boldsymbol{v} + \delta\boldsymbol{b} \cdot \delta\boldsymbol{b})\delta\boldsymbol{v} - 2(\delta\boldsymbol{v} \cdot \delta\boldsymbol{b})\delta\boldsymbol{b} \\
& - d_i(\delta\boldsymbol{b} \cdot \delta\boldsymbol{b})\delta\boldsymbol{j} + 2d_i(\delta\boldsymbol{b} \cdot \delta\boldsymbol{j})\delta\boldsymbol{b} \rangle \\
& + 2d_i \langle \delta\boldsymbol{j} \cdot \delta[(\boldsymbol{b} \cdot \nabla)\boldsymbol{b}] \rangle \\
& + 4\partial_t \langle E^{\text{tot}} \rangle - 2\langle \boldsymbol{v} \cdot \boldsymbol{d'}_\nu \rangle - 2\langle \boldsymbol{v}' \cdot \boldsymbol{d}_\nu \rangle \\
& - 2\langle \boldsymbol{b} \cdot \boldsymbol{d'}_\eta \rangle - 2\langle \boldsymbol{b}' \cdot \boldsymbol{d}_\eta \rangle - 2\langle \boldsymbol{v} \cdot \boldsymbol{f}' \rangle - 2\langle \boldsymbol{v}' \cdot \boldsymbol{f} \rangle.
\end{aligned} \tag{15}$$

It is interesting to note at this level that expression (15) is fully compatible with the limit $\ell \to 0$ since in this case each term of the first line tends to 0, and in the second line we have an exact compensation between the first term and the others by means of Equation (8)

The final expression of the exact law for 3D IHMHD, valid in the inertial range, is obtained by using the stationarity assumption and the limit of a wide inertial range (i.e., large kinetic/magnetic Reynolds numbers limit) for which

$$\langle \boldsymbol{v} \cdot \boldsymbol{d'}_\nu \rangle \simeq \langle \boldsymbol{v}' \cdot \boldsymbol{d}_\nu \rangle \simeq \langle \boldsymbol{b} \cdot \boldsymbol{d'}_\eta \rangle \simeq \langle \boldsymbol{b}' \cdot \boldsymbol{d}_\eta \rangle \simeq 0, \tag{16}$$

and also (with the properties of the external force)

$$\langle \boldsymbol{v} \cdot \boldsymbol{f}' \rangle \simeq \langle \boldsymbol{v}' \cdot \boldsymbol{f} \rangle \simeq \varepsilon. \tag{17}$$

We find the expression

$$\begin{aligned}
-4\varepsilon = & \nabla_\ell \cdot \langle (\delta\boldsymbol{v} \cdot \delta\boldsymbol{v} + \delta\boldsymbol{b} \cdot \delta\boldsymbol{b})\delta\boldsymbol{v} - 2(\delta\boldsymbol{v} \cdot \delta\boldsymbol{b})\delta\boldsymbol{b} \\
& - d_i(\delta\boldsymbol{b} \cdot \delta\boldsymbol{b})\delta\boldsymbol{j} + 2d_i(\delta\boldsymbol{b} \cdot \delta\boldsymbol{j})\delta\boldsymbol{b} \rangle \\
& - 2d_i \langle \delta\boldsymbol{j} \cdot \delta[(\boldsymbol{b} \cdot \nabla)\boldsymbol{b}] \rangle.
\end{aligned} \tag{18}$$

This law can be written in a compact form as

$$-4\varepsilon = \nabla_\ell \cdot (\boldsymbol{Y} + \boldsymbol{H}) - 2A, \tag{19}$$

where

$$\boldsymbol{Y} = \langle (\delta\boldsymbol{v} \cdot \delta\boldsymbol{v} + \delta\boldsymbol{b} \cdot \delta\boldsymbol{b})\delta\boldsymbol{v} - 2(\delta\boldsymbol{v} \cdot \delta\boldsymbol{b})\delta\boldsymbol{b} \rangle, \tag{20}$$

$$\boldsymbol{H} = d_i \langle 2(\delta\boldsymbol{b} \cdot \delta\boldsymbol{j})\delta\boldsymbol{b} - (\delta\boldsymbol{b} \cdot \delta\boldsymbol{b})\delta\boldsymbol{j} \rangle, \tag{21}$$

$$A = d_i \langle \delta\boldsymbol{j} \cdot \delta[(\boldsymbol{b} \cdot \nabla)\boldsymbol{b}] \rangle. \tag{22}$$

Here the contribution of the Hall effect is split into a flux $\boldsymbol{H}$ and a corrective term A. In the limit $d_i \to 0$ we recover the classic MHD law of Politano & Pouquet (1998a). Note that Equation (19) is the same as the one proposed in Hellinger et al. (2018), except for the corrective term A, which is multiplied here by a -2 factor (instead of 1). Assuming isotropy we can integrate expression (19), which leads to

$$-\frac{4}{3}\varepsilon\ell = Y_\ell + H_\ell - 2I_A, \tag{23}$$

where Y_ℓ and H_ℓ are the projections along the displacement direction ℓ, respectively, and $I_A = (1/\ell^2)\int_0^\ell r^2 A dr$.

Because the corrective term A can prove to be difficult to compute in spacecraft data due to the term $\delta[(\boldsymbol{b} \cdot \nabla)\boldsymbol{b}]$, we will see in the next section that H18 law can be improved and written using a simpler and more compact formulation involving only the $\boldsymbol{H}$ term.

3. Alternative Formulation of the Corrected H18

To improve the corrected H18 law we need to do some calculations on the term A. Using the fact that $\nabla(\boldsymbol{X} \cdot \boldsymbol{X}) = 2\boldsymbol{X} \times (\nabla \times \boldsymbol{X}) + 2(\boldsymbol{X} \cdot \nabla)\boldsymbol{X}$ and following a logic of calculation similar to Banerjee & Kritsuk (2018), we have

$$A = d_i \left\langle \delta\boldsymbol{j} \cdot \delta\left[\frac{1}{2}\nabla(\boldsymbol{b} \cdot \boldsymbol{b}) + \boldsymbol{j} \times \boldsymbol{b}\right]\right\rangle, \tag{24}$$

and, using derivative properties along with $\nabla \cdot \boldsymbol{j} = 0$, this equation reduces to

$$A = d_i \langle \delta\boldsymbol{j} \cdot \delta(\boldsymbol{j} \times \boldsymbol{b}) \rangle. \tag{25}$$

Now, with the relation $\nabla \cdot (\boldsymbol{X} \times \boldsymbol{Y}) = \boldsymbol{Y} \cdot (\nabla \times \boldsymbol{X}) - \boldsymbol{X} \cdot (\nabla \times \boldsymbol{Y})$ we can write (following Banerjee & Galtier 2017)

$$\begin{aligned}
\langle (\boldsymbol{j} \times \boldsymbol{b}) \cdot \boldsymbol{j}' \rangle &= \langle (\boldsymbol{j} \times \boldsymbol{b}) \cdot (\nabla' \times \boldsymbol{b}') \rangle \\
&= -\langle \nabla' \cdot [(\boldsymbol{j} \times \boldsymbol{b}) \times \boldsymbol{b}'] \rangle \\
&= -\nabla_\ell \cdot \langle (\boldsymbol{j} \times \boldsymbol{b}) \times \boldsymbol{b}' \rangle,
\end{aligned} \tag{26}$$

$$\langle (\boldsymbol{j}' \times \boldsymbol{b}') \cdot \boldsymbol{j} \rangle = \nabla_\ell \cdot \langle (\boldsymbol{j}' \times \boldsymbol{b}') \times \boldsymbol{b} \rangle, \tag{27}$$

$$\langle (\boldsymbol{j}' \times \boldsymbol{b}') \cdot \boldsymbol{j}' \rangle = \langle (\boldsymbol{j} \times \boldsymbol{b}) \cdot \boldsymbol{j} \rangle = 0, \tag{28}$$

which leads to

$$A = d_i \nabla_\ell \cdot \langle (\boldsymbol{j} \times \boldsymbol{b}) \times \boldsymbol{b}' - (\boldsymbol{j}' \times \boldsymbol{b}') \times \boldsymbol{b} \rangle. \tag{29}$$

Using identities for a double cross product, Equation (29) can be cast as

$$\begin{aligned}
A = & \frac{1}{2} d_i \nabla_\ell \cdot \langle 2(\delta\boldsymbol{b} \cdot \delta\boldsymbol{j})\delta\boldsymbol{b} - (\delta\boldsymbol{b} \cdot \delta\boldsymbol{b})\delta\boldsymbol{j} \rangle \\
& - d_i \nabla_\ell \cdot \langle (\boldsymbol{b} \cdot \boldsymbol{j}')\boldsymbol{b} - (\boldsymbol{b}' \cdot \boldsymbol{j})\boldsymbol{b}' \rangle \\
= & \frac{1}{2} \nabla_\ell \cdot \boldsymbol{H} \\
& + d_i \langle \boldsymbol{j}' \cdot [(\boldsymbol{b} \cdot \nabla)\boldsymbol{b}] + \boldsymbol{j} \cdot [(\boldsymbol{b}' \cdot \nabla')\boldsymbol{b}'] \rangle \\
= & \frac{1}{2} \nabla_\ell \cdot \boldsymbol{H} - A,
\end{aligned} \tag{30}$$

and we obtain

$$\nabla_\ell \cdot \boldsymbol{H} = 4A. \tag{31}$$

Injecting relation (31) into expression (19) we finally obtain the new formulation

$$-4\varepsilon = \boldsymbol{\nabla}_\ell \cdot \left(\boldsymbol{Y} + \frac{1}{2}\boldsymbol{H}\right), \tag{32}$$

which can be reduced to the following expression in the isotropic case:

$$-\frac{4}{3}\varepsilon\ell = Y_\ell + \frac{1}{2}H_\ell. \tag{33}$$

This new formulation, which will be referred to as F19 hereafter, is one of the main results of this paper. It has the double advantage of depending only on the product of increments of the physical fields (unlike the G08 model) and of being expressed only as flux terms. This makes it easier to apply in particular to single spacecraft data (under the assumption of isotropy).

Below we will verify whether the law (32) derived above is compatible with the other IHMHD laws (G08 and BG17) in the inertial range. The testing will be focused on the Hall-induced terms $\boldsymbol{H}$ and A, as the ideal MHD term $\boldsymbol{Y}$ is exactly the same as the one from Politano & Pouquet (1998b) and, by extension, the same as the ideal MHD component of G08. We will first investigate this question at the mathematical level and then with DNSs of EMHD.

4. Equivalence of the Exact Laws

4.1. Compatibility between F19 and G08

Here we show the equivalence of F19 and G08 by keeping only the Hall contributions. In G08, the law reads with our notation

$$-4\varepsilon_{\text{Hall}} = 4d_i \boldsymbol{\nabla}_\ell \cdot \langle(\boldsymbol{j} \times \boldsymbol{b}) \times \delta\boldsymbol{b}\rangle. \tag{34}$$

We already showed that $\boldsymbol{\nabla}_\ell \cdot \boldsymbol{H} = 4A$. With Equation (29) we have

$$\begin{aligned}\frac{1}{2}\boldsymbol{\nabla}_\ell \cdot \boldsymbol{H} &= 2d_i \boldsymbol{\nabla}_\ell \cdot \langle(\boldsymbol{j} \times \boldsymbol{b}) \times \boldsymbol{b}' - (\boldsymbol{j}' \times \boldsymbol{b}') \times \boldsymbol{b}\rangle \\ &= 4d_i \boldsymbol{\nabla}_\ell \cdot \langle(\boldsymbol{j} \times \boldsymbol{b}) \times \boldsymbol{b}'\rangle,\end{aligned} \tag{35}$$

which is enough to show that

$$\frac{1}{2}\boldsymbol{\nabla}_\ell \cdot \boldsymbol{H} = 4d_i \boldsymbol{\nabla}_\ell \cdot \langle(\boldsymbol{j} \times \boldsymbol{b}) \times \delta\boldsymbol{b}\rangle, \tag{36}$$

proving the compatibility.

4.2. Compatibility between G08 and BG17

Demonstrating the equivalence between the Hall terms of G08 and BG17 is even simpler. In the latter the Hall term is written

$$-4\varepsilon_{\text{Hall}} = 2d_i \langle\delta(\boldsymbol{j} \times \boldsymbol{b}) \cdot \delta\boldsymbol{j}\rangle. \tag{37}$$

Using Equations (25) and (31) we immediately obtain

$$\frac{1}{2}\boldsymbol{\nabla}_\ell \cdot \boldsymbol{H} = 2di\langle\delta(\boldsymbol{j} \times \boldsymbol{b}) \cdot \delta\boldsymbol{j}\rangle, \tag{38}$$

and thus prove the equivalence.

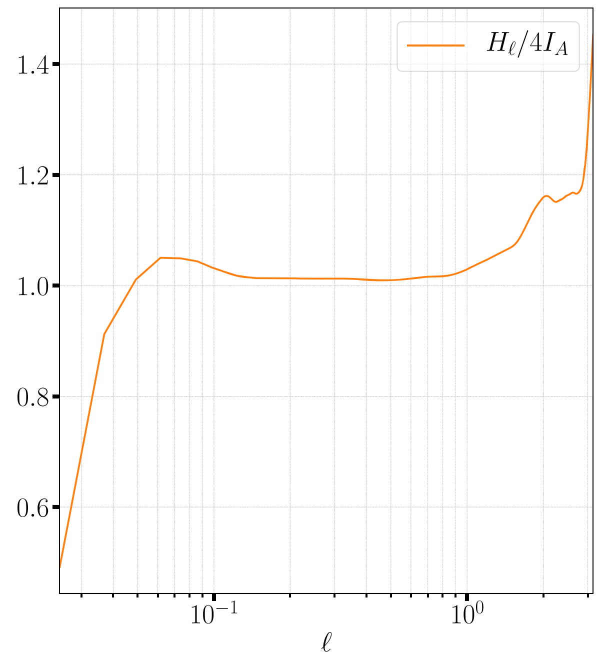

Figure 1. Ratio of H_ℓ to $4I_A$ of the F19 law.

5. Numerical Study

5.1. The Equivalence of the Models G08, BG17, and F19

In this section we will compare the G08, BG17, and F19 laws by using 3D DNSs of incompressible EMHD turbulence (Equations (4) with $\boldsymbol{v} = 0$). We used a modified version of the TURBO code (Teaca et al. 2009) in which we have implemented the Hall effect (Meyrand & Galtier 2013). The EMHD equations are solved in a triply periodic box. A pseudospectral algorithm is used to perform the spatial discretization on a grid with a resolution of 512^3 collocation points (see Meyrand & Galtier 2013 for further details). A mean guide field $\boldsymbol{b}_0$ of magnitude unity is introduced along the z axis. A large-scale forcing is applied that enforces a constant rate of energy injection with no helicity. The system is evolved until a stationary state is reached such that $\boldsymbol{b}_{\text{rms}} \sim \boldsymbol{b}_0$. We removed the amount of ideal invariants that is injected into the system by the forcing mechanism by means of magnetic hyperdiffusivity $\eta_3\Delta^3$ with $\eta_3 = 10e^{-11}$. The data consist of three periodic cubes giving the three components of the magnetic field in each grid point. The values of $\varepsilon_{\text{Hall}}$ are obtained by averaging the mixed field increments of the different exact laws over all the points of the data cubes and spherically integrating them, using for the increment vectors ℓ a set of specific directions in space defined by 73 base vectors as described in Taylor et al. (2003), and lengths going from a three point distance to half the size of the cubes (see also Andrés et al. 2018b).

First of all, we want to check numerically the new law F19 and, more precisely, the analytical relation found between H_ℓ and $4I_A$. In Figure 1 we represent $H_\ell/4I_A$, which shows differences mainly at large and small scales but not at intermediate scales where the inertial range is supposed to be. The differences observed are probably a consequence of the different nature of these two terms, being respectively a flux and an integrated term. The methods involved in the calculation being different, we can expect some minor differences. These should not alter the estimation of the energy cascade rate that is

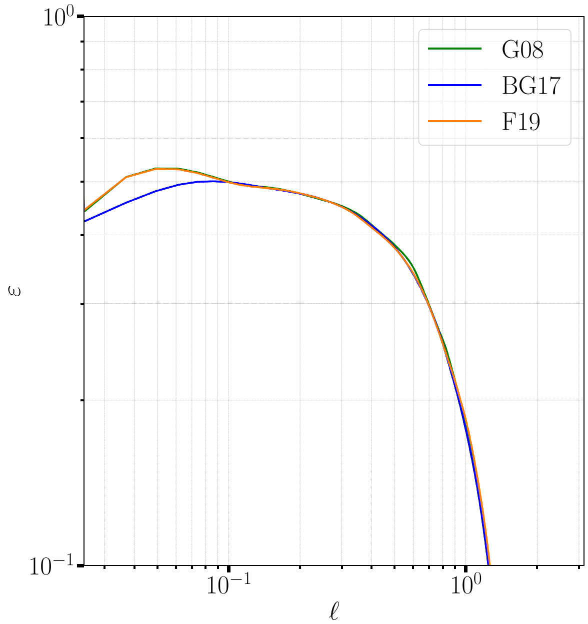

Figure 2. Energy cascade rates $\varepsilon_{\rm Hall}$ computed with F19, G08, and BG17.

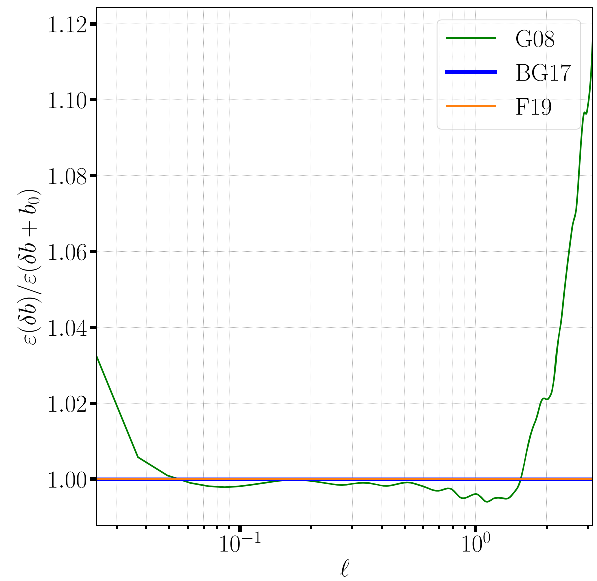

Figure 3. Ratios of $\varepsilon_{\rm Hall}$ computed from the data cubes where the guide field $\boldsymbol{b}_0$ is removed and from the data cubes where it is not. The values obtained with F19 and BG17 overlap.

measured in the inertial range, i.e., for scales $\ell \leqslant 0.3$ (see below).

To compare the three energy cascade rates obtained with the different expressions we first note that the Hall term in the G08 model can be written as

$$\mathrm{G08_{Hall}} = 2\boldsymbol{\nabla}_\ell \cdot \langle (\boldsymbol{j} \times \boldsymbol{b}) \times \delta\boldsymbol{b} + (\boldsymbol{j}' \times \boldsymbol{b}') \times \delta\boldsymbol{b} \rangle.$$

This formulation is chosen (over other possible expressions) because it ensures a symmetry between $\boldsymbol{x}$ and $\boldsymbol{x}'$ as in the two other laws, F19 and BG17. One must also be careful when computing BG17, as this law gives the energy cascade rate as a function of a direct statistical mean and not a flux, and thus does not require an integration a priori. However, we need to keep in mind that ε is not, in fact, exactly constant in our data. Consequently, when we integrate F19 and G08, we compute in reality $(1/\ell^3)\int_0^\ell r^2 \varepsilon dr$ and not ε. To remain consistent between the three models, we need to use the nonintegrated forms of both F19 and G08 ((32), (34)). This is what will be done hereafter.

We computed the energy cascade rate from the three laws and obtained the results gathered in Figure 2. All three laws fit remarkably well with each other, however, with a slightly different behavior of BG17 model at scales $\ell \leqslant 0.1$. Using the nonintegrated forms of G08 and F19 required us to apply a discrete derivation to our results as we only compute the inner bracket of the flux terms, and we expect this operation to be responsible for the differences at small scales due to a lack of resolution in this range of scales. The inertial range induced by the Hall effect is not easy to pinpoint precisely, but can be roughly estimated as going from 0.05 to 0.3 in this simulation.

5.2. On the Role of $\boldsymbol{b}_0$

Finally, we tested the influence of a guide field $\boldsymbol{b}_0$ on the estimation of $\varepsilon_{\rm Hall}$. Indeed, the introduction of a uniform magnetic field $\boldsymbol{b}_0$ into the previous laws does not change their expression. This is obvious for F19, which only depends on increments, and for BG17, in which the $\boldsymbol{b}_0$ influence translates as $\langle \delta\boldsymbol{j} \cdot ((\delta\boldsymbol{j}) \times \boldsymbol{b}_0)\rangle = 0$. For G08 we have

$$\begin{aligned}\mathrm{G08_{Hall}} &= 2\boldsymbol{\nabla}_\ell \cdot \langle (\boldsymbol{j} \times \boldsymbol{b}_0) \times \boldsymbol{b}' - (\boldsymbol{j}' \times \boldsymbol{b}_0) \times \boldsymbol{b} \rangle \\ &= -2\langle (\boldsymbol{j} \times \boldsymbol{b}_0) \cdot \boldsymbol{j}' + (\boldsymbol{j}' \times \boldsymbol{b}_0) \cdot \boldsymbol{j} \rangle \\ &= 0. \end{aligned} \quad (39)$$

Thus, when computing ϵ taking $\boldsymbol{b}_0$ into account or not in the data should not affect the result. However, for practical reasons related to the numerical computation, $\boldsymbol{b}_0$ may have some influence on estimating ϵ as we show now.

Values of $\varepsilon_{\rm Hall}$ computed only with the fluctuating magnetic fields were obtained by averaging the magnetic field component along the guide field axis (here the z axis) and subtracting this value from that component. In Figure 3 we see that computing the energy cascade rate with or without the mean guide field leads to the same result for all but G08, even though the contribution of $\boldsymbol{b}_0$ reduces to zero mathematically. The difference is, however, very small in the inertial range (less than 0.5%).

We believe this problem to be tied to the way we handle derivatives. F19 is formed of only increments and so does not involves $\boldsymbol{b}_0$, unlike the models BG17 and G08 that contain a $\boldsymbol{b}_0$ contribution a priori, but whose contributions in fact reduce to zero. However, from these contributions, only the one in G08 comes from a flux term and so is preceded by a derivative. When we compute numerically the energy cascade rates we do not really calculate this derivative but rather use the approximation $\boldsymbol{\nabla}_\ell \rightarrow 1/\ell$. Thus, we are making an approximation in the calculation and this may be the cause of the behavior shown in Figure 3. A similar remark was made in Hadid et al. (2017), which led us to this conclusion. It may also be worth mentioning that the validity of this approximation is tied to the validity of the hypotheses of isotropy and homogeneity, and the influence of $\boldsymbol{b}_0$ would probably be more important when using observational data where these hypotheses are harder to meet.

Based on these remarks and on the behavior of the three laws we conclude that, as expected, $\boldsymbol{b}_0$ does not contribute explicitly to the incompressible energy cascade rate and, in the purpose of computing $\varepsilon_{\text{Hall}}$, that it should be removed from the simulation of the spacecraft data beforehand in order to minimize the possible numerical errors that it can generate. Note that this property does not mean that $\boldsymbol{b}_0$ has no influence on the nonlinear dynamics (Galtier et al. 2000; Wan et al. 2012; Oughton et al. 2013): it is actually expected that the energy cascade rate $\varepsilon_{\text{Hall}}$ decreases with increasing b_0, as shown recently with DNSs (Bandyopadhyay et al. 2018). It is worth mentioning that the situation is very different in compressible law (e.g., Banerjee & Galtier 2013) where the $\boldsymbol{b}_0$ dependence is explicit and cannot a priori be ruled out (Hadid et al. 2017). However, recent developments suggest that its influence will not be significant as it mostly impacts the volumic contributions to the law, which appear to be small compared to the dominant flux terms (Andrés et al. 2018b).

6. Conclusion

The energy cascade rate ε is an essential tool for studying turbulent flows. Despite being sometimes hard to compute it can be theoretically calculated by several equivalent formulations. We showed here that the law (19), which is obtained using the same premises as proposed in Hellinger et al. (2018), can be written (when corrected) in a compact form with only a flux term (32). As shown numerically, this gives the same energy cascade rate in the inertial range as with the G08 and BG17 laws. This diversity of exact laws gives more freedom to compute the energy cascade rate of IHMHD turbulence as it is possible to adapt the computation method to the data available and their quality.

For instance, we showed that the presence of a mean guide field should not contribute explicitly to the energy cascade rate. This theoretical property is well verified with DNSs for BG17 and F19, but not for G08, which shows a dependence on $\boldsymbol{b}_0$ that can be interpreted as residual errors due to the performed computation. Although this dependence remains small in the present paper, it is more important in spacecraft data analysis (N. Andrés 2019, private communication). Therefore, we advise using F19 or BG17 laws to compute the energy cascade rate as they are free from the errors induced by the presence of a mean guide field.

The authors acknowledge financial support from CNRS/CONICET Laboratoire International Associé (LIA) MAGNETO. N.A. is supported through a DIM-ACAV post-doctoral fellowship. S.B. acknowledges DST Inspire research grant.

ORCID iDs

S. Galtier https://orcid.org/0000-0001-8685-9497
N. Andrés https://orcid.org/0000-0002-1272-2778
S. Banerjee https://orcid.org/0000-0002-3746-0989

References

Andrés, N., Galtier, S., & Sahraoui, F. 2018a, PhRvE, 97, 013204
Andrés, N., & Sahraoui, F. 2017, PhRvE, 96, 053205
Andrés, N., Sahraoui, F., Galtier, S., et al. 2018b, JPlPh, 84, 905840404
Antonia, R., Ould-Rouis, M., Anselmet, F., & Zhu, Y. 1997, JFM, 332, 395
Bandyopadhyay, R., Oughton, S., Wan, M., et al. 2018, PhRvX, 8, 041052
Banerjee, S., & Galtier, S. 2013, PhRvE, 87, 013019
Banerjee, S., & Galtier, S. 2014, JFM, 742, 230
Banerjee, S., & Galtier, S. 2016, PhRvE, 93, 033120
Banerjee, S., & Galtier, S. 2017, JPhA, 50, 015501
Banerjee, S., Hadid, L., Sahraoui, F., & Galtier, S. 2016, ApJL, 829, L27
Banerjee, S., & Kritsuk, A. G. 2017, PhRvE, 96, 053116
Banerjee, S., & Kritsuk, A. G. 2018, PhRvE, 97, 023107
Batchelor, G. 1953, The Theory of Homogeneous Turbulence (Cambridge: Cambridge Univ. Press)
Carbone, V., Marino, R., Sorriso-Valvo, L., Noullez, A., & Bruno, R. 2009, PhRvL, 103, 061102
Coburn, J., Forman, M., Smith, C., Vasquez, B., & Stawarz, J. 2015, RSPTA, 373, 20140150
Duchon, J., & Robert, R. 2000, Nonli, 13, 249
Eyink, G. L. 1994, PhyD, 78, 222
Frisch, U. 1995, Turbulence (Cambridge: Cambridge Univ. Press)
Galtier, S. 2008, PhRvE, 77, 015302
Galtier, S. 2016, Introduction to Modern Magnetohydrodynamics (Cambridge: Cambridge Univ. Press)
Galtier, S. 2018, JPhA, 51, 205501
Galtier, S., & Banerjee, S. 2011, PhRvL, 107, 134501
Galtier, S., Nazarenko, S., Newell, A., & Pouquet, A. 2000, JPlPh, 63, 447
Hadid, L., Sahraoui, F., & Galtier, S. 2017, ApJ, 838, 9
Hadid, L. Z., Sahraoui, F., Galtier, S., & Huang, S. Y. 2018, PhRvL, 120, 055102
He, J., Wang, L., Tu, C., Marsch, E., & Zong, Q. 2015, ApJL, 800, L31
Hellinger, P., Verdini, A., Landi, S., Franci, L., & Matteini, L. 2018, ApJL, 857, L19
Kolmogorov, A. 1941, DoSSR, 32, 16
MacBride, B., Smith, C., & Forman, M. 2008, ApJ, 679, 1644
Marino, R., Sorriso-Valvo, L., Carbone, V., et al. 2008, ApJL, 677, L71
Matthaeus, W. H., Zank, G. P., Smith, C. W., & Oughton, S. 1999, PhRvL, 82, 3444
Meyrand, R., & Galtier, S. 2013, PhRvL, 111, 264501
Mininni, P. D., & Pouquet, A. 2009, PhRvE, 80, 025401
Monin, A. S. 1959, Doklady Akademii Nauk SSSR, 125, 515
Onsager, L. 1949, NCim, 6, 279
Osman, K. T., Wan, M., Matthaeus, W. H., Weygand, J. M., & Dasso, S. 2011, PhRvL, 107, 165001
Oughton, S., Wan, M., Servidio, S., & Matthaeus, W. H. 2013, ApJ, 768, 10
Podesta, J. J., Forman, M. A., & Smith, C. W. 2007, PhPl, 14, 092305
Politano, H., & Pouquet, A. 1998a, PhRvE, 57, 21
Politano, H., & Pouquet, A. 1998b, GeoRL, 25, 273
Richardson, J. D., Paularena, K. I., Lazarus, A. J., & Belcher, J. W. 1995, GeoRL, 22, 325
Sahraoui, F., Goldstein, M. L., Belmont, G., Canu, P., & Rezeau, L. 2010, PhRvL, 105, 131101
Sahraoui, F., Goldstein, M. L., Robert, P., & Khotyaintsev, Y. V. 2009, PhRvL, 102, 231102
Saint-Michel, B., Herbert, E., Salort, J., et al. 2014, PhFl, 26, 125109
Smith, C. W., Stawarz, J. E., Vasquez, B. J., Forman, M. A., & MacBride, B. T. 2009, PhRvL, 103, 201101
Sorriso-Valvo, L., Marino, R., Carbone, V., et al. 2007, PhRvL, 99, 115001
Stawarz, J. E., Smith, C. W., Vasquez, B. J., Forman, M. A., & MacBride, B. T. 2009, ApJ, 697, 1119
Taylor, M. A., Kurien, S., & Eyink, G. L. 2003, PhRvE, 68, 026310
Teaca, B., Verma, M. K., Knaepen, B., & Carati, D. 2009, PhRvE, 79, 046312
Wan, M., Oughton, S., Servidio, S., & Matthaeus, W. H. 2012, JFM, 697, 296